

# Journal of Bioactive and Compatible Polymers

<http://jbc.sagepub.com/>

---

## Hybrid biodegradable membranes of silane-treated chitosan/soy protein for biomedical applications

Simone S Silva, Joaquim M Oliveira, Johan Benesch, Sofia G Caridade, João F Mano and Rui R Reis

*Journal of Bioactive and Compatible Polymers* published online 14 June 2013  
DOI: 10.1177/0883911513490361

The online version of this article can be found at:  
</content/early/2013/06/11/0883911513490361>

---

Published by:



<http://www.sagepublications.com>

Additional services and information for *Journal of Bioactive and Compatible Polymers* can be found at:

**Email Alerts:** </cgi/alerts>

**Subscriptions:** </subscriptions>

**Reprints:** <http://www.sagepub.com/journalsReprints.nav>

**Permissions:** <http://www.sagepub.com/journalsPermissions.nav>

>> [OnlineFirst Version of Record](#) - Jun 14, 2013

[What is This?](#)

# Hybrid biodegradable membranes of silane-treated chitosan/soy protein for biomedical applications

Journal of Bioactive and  
Compatible Polymers

0(0) 1–13

© The Author(s) 2013

Reprints and permissions:

sagepub.co.uk/journalsPermissions.nav

DOI: 10.1177/0883911513490361

jbc.sagepub.com



**Simone S Silva<sup>1,2</sup>, Joaquim M Oliveira<sup>1,2</sup>, Johan Benesch<sup>1,2</sup>,  
Sofia G Caridade<sup>1,2</sup>, João F Mano<sup>1,2</sup> and Rui R Reis<sup>1,2</sup>**

## Abstract

In recent years, progress in the field of hybrid materials has been accelerated through use of the sol–gel process for creating materials and devices, which benefit from the incorporation of both inorganic and organic components. In this work, organic–inorganic hybrid membranes were prepared from tetraethoxysilane and a blend system composed of chitosan and soy protein. By introducing a small amount of siloxane bond into the chitosan/soy protein system, the chitosan/soy protein hybrid membranes were improved in terms of structure, topography and mechanical properties. It appears that the chitosan/soy protein hybrid membranes were formed by discrete inorganic moieties entrapped in the chitosan/soy protein blend, which improved the stability and mechanical performance assessed by the dynamic mechanical analysis as compared to chitosan/soy protein membrane. Also, *in vitro* cell culture studies evidenced that the chitosan/soy protein hybrid membranes are non-cytotoxic over a mouse fibroblast-like cell line. The hybrid membranes of silane-treated chitosan/soy protein developed in this work have potential in biomedical applications, including tissue engineering.

## Keywords

Soy protein, hybrid materials, chitosan, biomaterials, tetraethoxysilane

<sup>1</sup>3B's Research Group- Biomaterials, Biodegradables and Biomimetics, University of Minho, Headquarters of the European Institute of Excellence on Tissue Engineering and Regenerative Medicine, AvePark, Zona Industrial da Gandra, Caldas das Taipas, 4806-909 Guimarães, Portugal

<sup>2</sup>ICVS/3B's- PT Government Associate Laboratory, Braga/Guimarães, Portugal

## Corresponding author:

Simone S Silva, 3B's Research Group- Biomaterials, Biodegradables and Biomimetics, University of Minho, Headquarters of the European Institute of Excellence on Tissue Engineering and Regenerative Medicine, AvePark, Zona Industrial da Gandra, Caldas das Taipas, 4806-909 Guimarães, Portugal.

Email: simonesilva@dep.uminho.pt

## Introduction

There is a growing interest in the use of sol–gel method for the creation of nanocomposites, biosensors and optical devices.<sup>1–3</sup> The sol–gel process has been used in the production of hybrid organic–inorganic materials, and represents a promising class of engineered materials, which includes functional and structural components constructed by the integration of biopolymers with inorganic components in a variety of forms.<sup>4–7</sup> Silane coupling agents such as 3-isocyanatopropyltriethoxysilane (ICPTES), 3-glycidyloxypropyltrimethoxysilane (GPTMS), 3-aminopropyltriethoxysilane (APTES) and tetraethoxysilane (TEOS)<sup>3,4,8,9</sup> have been used to form the inorganic component of the hybrid materials, while natural polymers and their blends have been considered good candidates to form the organic phase due to their intrinsic properties and characteristics.<sup>10</sup> Among the different polymers included in sol–gel matrices<sup>4,6</sup> chitin/chitosan and their blend appears to be good base materials due to their relatively facile modification and suitability for technological applications.<sup>10–13</sup> These offer several ways to construct materials with a broad range of properties, potentially suiting them for use in pharmaceutical, biomedical and cosmetic applications.

This work focused on the creation of a set of chitosan/soy protein hybrid (CSH) membranes prepared by means of a sol–gel process using the TEOS and chitosan/soy protein (CS)-blend system as the inorganic and organic components, respectively. In previous works,<sup>14,15</sup> the CS system was found to be adequate to create scaffolds and membranes for finding application in cartilage regeneration and as wound dressing. Therefore, the CS system may be a promising candidate for applications in the field of regenerative medicine. However, problems may arise due to the immiscibility of the two phases.<sup>16</sup> We hypothesized that the silanization treatment and formation of siloxane domains, promoted by an in situ sol–gel process, would increase the interfacial interactions between the two phases. To test this hypothesis, the effect of TEOS/HCl ratio on the developed hybrid membranes was evaluated, along with the stability, morphology, mechanical and structural properties. To investigate the possible cytotoxic effect of the new materials, both CS and CSH extracts were placed in contact with fibroblast-like cells (L929), and a cellular viability assay (3-(4, 5-dimethylthiazol-2-yl)2, 5-diphenyl tetrazolium bromide (MTT)) was performed.

## Materials and methods

Chitosan (medium molecular weight, CAS 9012-76-4; Sigma–Aldrich, Germany) was purified by a re-precipitation method.<sup>17</sup> The deacetylation degree of chitosan was about 84%, determined by Proton Nuclear Magnetic Resonance (<sup>1</sup>H-NMR) spectroscopy.<sup>18</sup> Soy protein isolate was provided by Loders Croklaan, the Netherlands. Soy protein isolate has a protein content of 90–91% (dry basis) and an isoelectric point of 4.2–4.5; and TEOS (99.999%), the inorganic constituent, was purchased from Sigma–Aldrich, and was used without purification. All other reagents were of analytical grade and used as received.

### *Preparation of CS-based hybrid membranes*

CS protein–blend solutions were prepared as described previously.<sup>15</sup> Briefly, chitosan flakes were dissolved in an aqueous acetic acid (0.2 M) at a concentration of 4 wt% (w/v) to obtain a homogeneous solution. A 1 wt% (w/v) soy suspension was prepared by slow stirring the soy protein

powder in distilled water glycerol solution (water/glycerol ratio 1:10). After adjusting the pH to  $8.0 \pm 0.3$  with 1 M NaOH solution, the dispersion was heated in a water bath at  $50^\circ\text{C}$  for 30 min. The two solutions were then mixed at CS75 ratio, corresponding to 75/25 w/w (chitosan/soy). After that, TEOS:0.5 M hydrochloric acid (HCl) ratio of 1:1 wt% and 1:0.1 wt% was added to CS, and the systems were kept at room temperature ( $25^\circ\text{C}$ ) under stirring for 24 h. The blended solutions were cast into petri dishes and dried at room temperature for 4 days. The neutralization of the hybrid membranes was then performed by soaking them in a 0.1 M NaOH solution for 10 min, followed by washing with distilled water until pH 7. The resulting membranes were dried at room temperature, and named as CSH1 and CSH2, where 1 and 2 indicate the 1:1 wt% and 1:0.1 wt% TEOS:HCl ratios added to the CS blend, respectively.

## Characterization

### *Fourier transform infrared with attenuated total reflection (FTIR-ATR)*

Surface changes on membranes were assessed by FTIR-ATR spectroscopy<sup>19</sup> (Uican Mattson 7000 FTIR spectrometer). All spectra were acquired at room temperature by averaging 64 scans at a resolution of  $4\text{ cm}^{-1}$ .

### *X-ray photoelectron spectroscopy (XPS)*

The XPS analysis was performed using an ESCALAB 200A, VG Scientific, with PISCES software for data acquisition and analysis. For analysis, an achromatic Al ( $K\alpha$ ) X-ray source operating at 15 kV (300 W) was used. The spectrometer calibrated with reference to Ag 3d<sub>5/2</sub> (368.27 eV) was operated in Constant Analyzer Energy (CAE) mode with 20-eV pass energy. XPS take-off angle was  $90^\circ$  (normal to the surface). Data acquisition was performed with a pressure lower than  $10^{-6}$  Pa. The value of 285 eV of the hydrocarbon C1s core level was used as a calibration for the absolute energy scale. Overlapping peaks were resolved into their individual components by use of XPSPEAK 4.1 software.

### *Scanning electron microscopy (SEM)*

The SEM images were obtained at 10 kV on a Leica Cambridge S-360 microscope equipped with a LINK eXLII X-ray energy dispersion spectrometer for silicon microanalysis.

### *Atomic force microscopy*

The samples were measured on at least three spots using TappingMode™ with a MultiMode connected to a NanoScope, both supplied from Veeco, New York, USA, with non-contacting silicon nanoprobes (ca 300 kHz, setpoint 2–3 V) purchased from Nanosensors, Switzerland. All images (10  $\mu\text{m}$  wide) were fitted to a plane using the third-degree flatten procedure included in the NanoScope software version 4.43r8. The surface roughness was calculated as Sq (root mean square from average flat surface) and Sa (average absolute distance from average flat surface). The values are presented as mean (standard deviation).

### Contact angle measurements

The surface properties of the membranes were also investigated by means of static contact angle ( $\theta$ ) measurements using the sessile drop method<sup>20</sup> with ultra-pure distilled water (polar) and diiodomethane (non-polar) (OCA equipment, Germany and SCA-20 software). Six measurements were carried out for each sample. The presented data (Table 2) are average of six measurements. The surface energy was calculated using the Owens, Wendt, Rabel and Kaelble (OWRK) equation.<sup>21</sup>

### Dynamic mechanical analysis

The viscoelastic measurements of the CS and CSH membranes were performed using a TRITEC2000B dynamic mechanical analysis (DMA) from Triton Technology, equipped with the tensile mode. The measurements were carried out in dry state and at room temperature. The distance between the clamps was 10 mm, and the membrane samples were cut into ~4 mm widths. DMA spectra were obtained during a frequency scan between 0.1 and 10 Hz. The experiments were performed under constant strain amplitude (30  $\mu\text{m}$ ). The average value of four tests was reported for each sample.

### Degradation and swelling assays

Degradation and water uptake of the CS and CSH membranes were evaluated through their immersion in phosphate buffer saline (PBS) (Sigma–Aldrich, Germany) at 37°C for a period up to 30 days. The weight of the swollen samples was measured after removing the excess of surface water by gently tapping the surface with filter paper. The percentage of water uptake was calculated using equation (1), where  $W_s$  is the swollen sample weight and  $W_d$  is the dry sample weight. Each experiment was repeated three times, and the average value was considered to be the water uptake value.

$$\text{Water uptake (\%)} = \left[ \frac{(W_s - W_d)}{W_d} \right] \times 100 \quad (1)$$

The percentage of weight loss was calculated using equation (2), where  $W_i$  and  $W_d$  correspond to the initial weight and dried sample weight, respectively.

$$\text{Weight loss (\%)} = \left[ \frac{(W_i - W_d)}{W_i} \right] \times 100 \quad (2)$$

### Cytotoxicity screening

Prior to cell culture studies, all membranes were sterilized under an ethylene oxide atmosphere. In order to assess the eventual cytotoxicity of the developed CS membranes, extracts of all membranes were prepared and placed in contact with the mouse fibroblast-like cell line L929 (L929 cells; European Collection of Cell Cultures (ECACC), UK) and tested using an MTT-based colorimetric assay<sup>22</sup> in accordance with the protocol described in ISO/EN 10993.<sup>23</sup> For these tests, cells were cultured in basic medium containing Dulbecco's modified Eagle's medium (DMEM; Sigma–Aldrich, USA) with phenol red supplemented with 10% fetal bovine serum (FBS; Gibco, UK) and

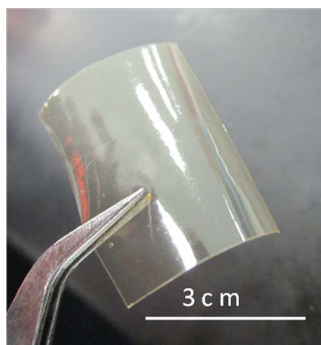


**Figure 1.** Representative photograph of the CSH membranes.  
CSH: chitosan/soy protein hybrid.

1% antibiotic/antimycotic (A/B; Gibco) solution. The extracts of the membranes were prepared as described previously.<sup>24</sup> Briefly, the membranes were immersed in culture medium for 24 h at 37°C and 60 r min<sup>-1</sup>. The filtered extracts were placed in contact with a monolayer of L929 cells for 72 h. The relative cell viability (%) of the L929 cells was determined for each CS extract, and compared to latex extracts used as a positive control of cell death.

## Statistical analysis

All quantitative experiments are run in triplicate, and results are expressed as mean  $\pm$  standard deviation for  $n = 3$ . Statistical analysis of the data was conducted using two-way analysis of variance (ANOVA) with Bonferroni's post-test by using GraphPad Prism version 5.0 for Windows (GraphPad Software, San Diego, CA, USA; <http://www.graphpad.com>). The following factors were used for the various types of characterization in the study: degradation time/weight loss/water uptake for degradation tests; + Sq/Sa for roughness and the %Si, %N and %C of the CSH membranes compared to CS used as a control for composition analysis. Differences between the groups with  $p < 0.05$  were considered to be statistically significant.

## Results

Inorganic–organic hybrid (CSH) membranes were successfully prepared by an in situ sol–gel process through hydrolysis and condensation of TEOS into CS-blend system. The CSH membranes obtained had a yellowish colour and were 78–120  $\mu\text{m}$  thick (Figure 1). No phase separation of the organic and inorganic phases was detected at a macroscopic level.

FTIR spectra of both modified and unmodified membranes are presented in Figure 2. The band characteristics of chitosan were observed around 1650  $\text{cm}^{-1}$  (amide I), 1565  $\text{cm}^{-1}$  (amide II) and 1150–1040  $\text{cm}^{-1}$  (C–O–C– in glycosidic linkage),<sup>25</sup> while soy protein was detected at 1632  $\text{cm}^{-1}$  (amide I) and at 1536  $\text{cm}^{-1}$  (amide II).<sup>26</sup> The presence of Si–O–Si stretching bands for the CSH hybrids in the region of 1000–1100  $\text{cm}^{-1}$  was also detected.<sup>27</sup> Nevertheless, the Si–O–Si linkage appears overlapped by the glycosidic linkage of chitosan, which occurred in the range of 1150–1040  $\text{cm}^{-1}$ .<sup>25</sup> The appearance of a shoulder peak at 945  $\text{cm}^{-1}$  (Si–O stretching)<sup>28</sup> was observed in the spectra of hybrid membranes, indicating the presence of silanol (Si–OH) groups.

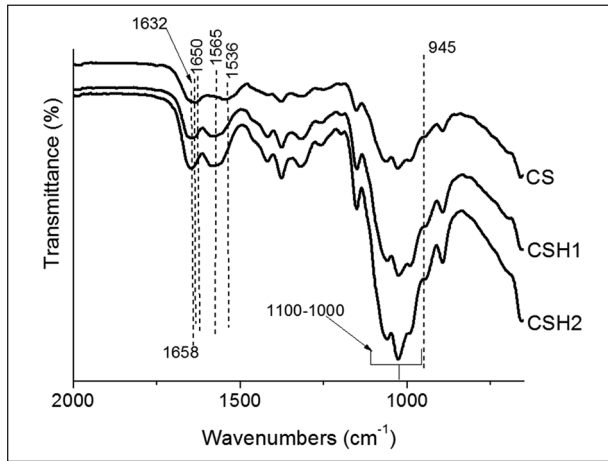


**Figure 2.** FTIR spectra of CS, CSH1 and CSH2 membranes.  
CS: chitosan/soy protein; CSH: chitosan/soy protein hybrid.

**Table 1.** Relative surface composition and atomic ratios determined by XPS analysis for unmodified and hybrid membranes.

Membrane	Surface composition				Atomic ratio (%)	
	%C	%O	%N	%Si	C/O ratio	O/Si ratio
CS	61.7	26.7	10	0.5	2.3	13.4
CSH1	64.6	26.1	4.8*	3.4*	2.5	7.7
CSH2	62.7	26.7	6.4*	3.6*	2.3	7.4

\* $p \leq 0.05$ .

XPS analysis was performed to determine the changes in surface elemental composition of the unmodified and modified membranes. As it can be seen from Table 1, silicon (Si) element was present in all hybrid membranes at different percentages. In CS membrane, the small Si percentage (0.5%) could be a result of the processing of the exoskeleton components from the source material.<sup>29</sup> The CSH membranes had a decrease in %N and an increase in both %C and %Si contents compared to unmodified CS membranes (Table 1). A  $p \leq 0.05$  was observed for %Si and %N when compared to CS.

### Surface topography

SEM images of the hybrid membranes did not show significant alterations of the surface morphology compared to the unmodified membranes (data not shown). The changes on the surface topography at nanometre levels of the hybrid membranes were studied by atomic force microscopy (AFM) (Figure 3). The inorganic phase in the CSH surfaces was homogeneously dispersed (CSH1, Figure 3(b); CSH2, Figure 3(c)) in the organic phase. From AFM data, an

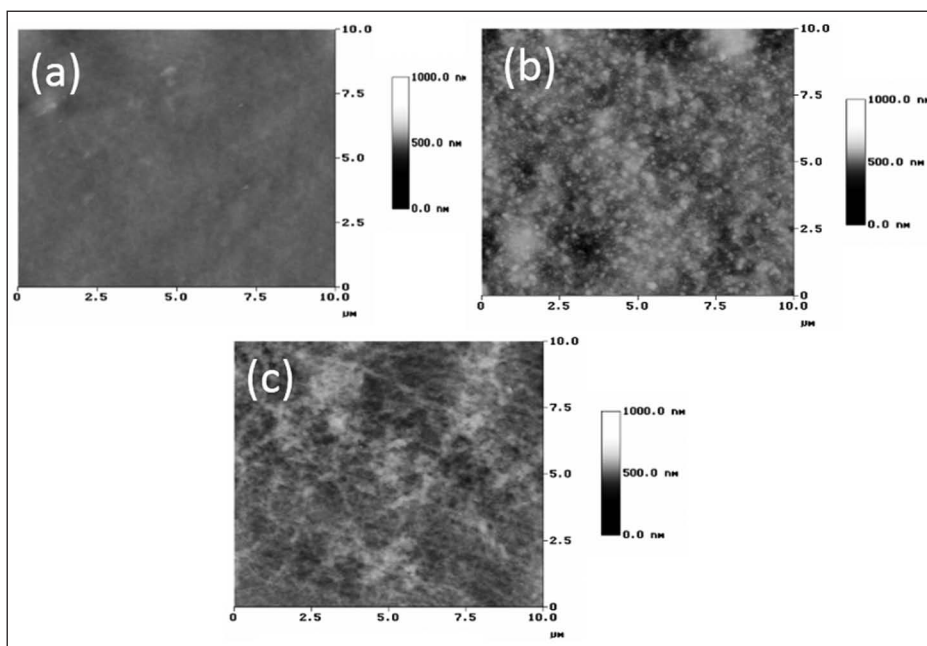


**Figure 3.** AFM images of the prepared membranes: (a) CS, (b) CSH1 and (c) CSH2 membranes.

increasing surface roughness at nanoscale level was observed as compared to CS in the hybrid membranes, from  $5.8 \pm 1.1$  (CS),  $7.0 \pm 1.9$  (CSH1) to  $14.6 \pm 5.3$  nm (CSH2). The presence of silica domains randomly dispersed in the CSH membranes may have contributed to these findings.

### Swelling and degradation behaviour

Water absorption ability and weight loss of the membranes were evaluated by monitoring the changes in PBS (pH 7.4) for up to 30 days. All the membranes were found to be stable in the PBS solution but had different water uptake and degradation profiles (Figure 4). Compared to the CS membrane, the CSH membranes showed less swelling (Figure 4(a)). This may be related to enhanced interaction between the protein and the polymer arising from the introduction of inorganic phase, with the inorganic network hindering the swelling through the contraction effects of the silica bridging bonds. Ren et al.<sup>9</sup> observed similar results in gelatin–siloxane hybrids. Statistical analysis of the water uptake data evidenced significant differences ( $p < 0.05$ ) at 21 and 30 days between CS and both CSH membranes. The degradation profile of both CS and CSH membranes involved the leaching of plasticizer (glycerol) and the loss of some protein fraction, followed by weight loss of the material (Figure 4(b)). A positive influence of the silica network in the CS system on degradation behaviour was evident in the CSH1 membranes, with their rate of weight loss being reduced. Statistical analysis of the weight loss data showed significant differences ( $p < 0.05$ ) between the CS and both CSH samples (CSH1 and CSH2) at prolonged degradation times (2 and 4 weeks).



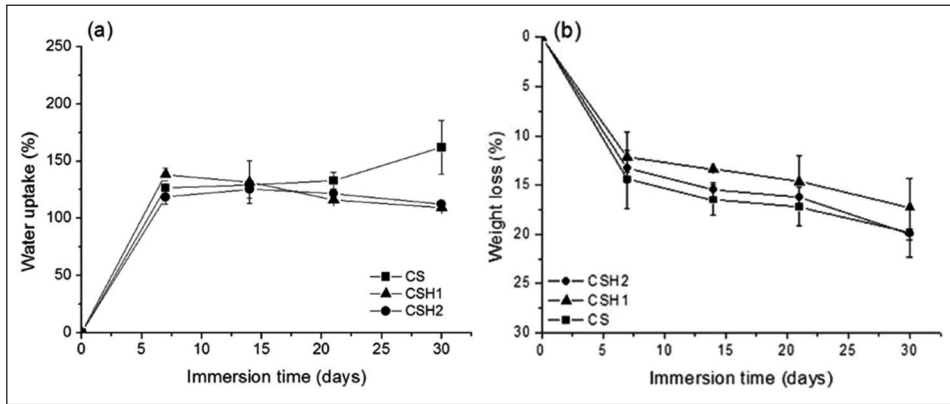


**Figure 4.** (a) Water uptake and (b) weight loss of the unmodified CS and CSH membranes with time in PBS at 37°C. Data represent the mean  $\pm$  standard deviation ( $p < 0.05$ , two-way ANOVA).

**Table 2.** Contact angles ( $\theta$ ), dispersive ( $\gamma_d$ ) and polar ( $\gamma_p$ ) components and superficial energy ( $\gamma$ ) of the prepared membranes calculated by the Owens–Wendt equation.

Membrane	$\theta_{water}$ ( $^\circ$ )	$\gamma_d$ (mN m $^{-1}$ )	$\gamma_p$ (mN m $^{-1}$ )	$\gamma$ (mN m $^{-1}$ )
CS	117.9 $\pm$ 4.6	17.6 $\pm$ 0.5	0.3 $\pm$ 0.02	17.9 $\pm$ 0.5
CSH1	97.3 $\pm$ 2.0	30.8 $\pm$ 0.4*	0.8 $\pm$ 0.03	31.6 $\pm$ 0.2*
CSH2	80.8 $\pm$ 1.4	27.4 $\pm$ 0.2*	5.0 $\pm$ 0.3*	32.4 $\pm$ 0.5*

\* $p \leq 0.05$  when compared to CS.

### Hydrophilic/hydrophobic balance and mechanical properties

The induced changes in the surface chemistry influence the hydrophilicity of the obtained membranes, which in turn may alter their bioactivity. The measured contact angles and the calculated surface energy of the studied materials are summarized in Table 2. The average water contact angles of the membranes decreased after sol–gel processing when compared to the unmodified CS membranes.

The surface energy was calculated using the method proposed by Owens et al.<sup>21</sup> As can be seen in Table 2, both hybrid membranes had lower contact angle values and significantly higher superficial energy ( $\gamma$ ). It is known that the contact angle depends on both the chemical composition of the surface and the surface roughness of the matrix.<sup>30</sup> Since both hybrid membranes showed increased surface roughness compared to CS, it may be assumed that the observed changes in contact angle were due to the altered chemical composition.

With respect to the mechanical properties, the storage modulus ( $E'$ ) and loss factor ( $\tan \delta$ ) of the unmodified CS and CSH membranes were plotted against frequency as shown in Figure 5. A small increase in  $E'$  with increasing frequency is verified for all samples (Figure 5(a)). The  $E'$  values of

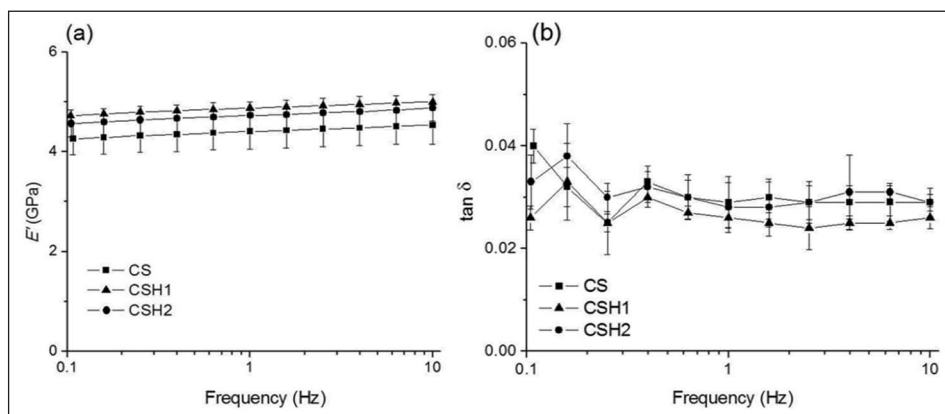


**Figure 5.** (a) Storage modulus ( $E'$ ) and (b) loss factor ( $\tan \delta$ ) of CS and CSH membranes obtained during frequency scans between 0.1 and 10 Hz in dry conditions at room temperature.

the CSH membranes are higher than those found for the CS membranes. The loss factor ( $\tan \delta$ ) measures the damping properties of the samples and provides an indication of its viscoelastic characteristics.<sup>31</sup> The frequency dependence on the  $\tan \delta$  values of the prepared membranes can be seen in Figure 5(b). Values between 0.04 and 0.03 were found, indicating that the damping properties of the CSH membranes do not exhibit significant variation compared with those of the CS membranes. These results also indicated that a relaxation process takes place in the membranes within the frequency range analyses.

### Cytotoxicity assays

The cytotoxicity of matrices was quantified using an MTT assay, which provides data on the metabolic activity of the cells when exposed to the leached out materials from the matrices.<sup>29</sup> After 3 days of incubation of L929, the effects of extracts of the membranes on cell growth were analysed. Cell viability values were  $96.5 \pm 4.8\%$ ,  $84.1 \pm 4.1\%$ ,  $92.9 \pm 4.6\%$  and  $98 \pm 0.5\%$  for CS, CSH1, CSH2 and control, respectively. Thus, the cell viability values for CSH membranes were nearly equivalent to those for CS membranes. All these results indicated that L929 cells have good cell viability, when compared to L929 in control wells.

### Discussion

The sol-gel process led to the formation of silanol groups ( $\equiv\text{Si-OH}$ ) with siloxane bonding ( $\text{Si-O-Si}$ ). These groups can interact with other functional groups present in the CS blend through dehydration or dealcoholysis reaction with other silanol or ethoxy groups during the solvent evaporation of the membrane formation process.<sup>32</sup> In this case, the acidic media in the CS-blended system can favour the hydrolysis of TEOS over condensation.<sup>33,34</sup> Shchipunov<sup>8</sup> found that the silanol groups produced after the hydrolysis of the precursor can form hydrogen bonds with the corresponding groups of biopolymers. Thus, the chitosan and soy protein blend could then form hydrogen-bonded bridges between adjacent silica particles between the polar groups on chitosan<sup>32</sup>

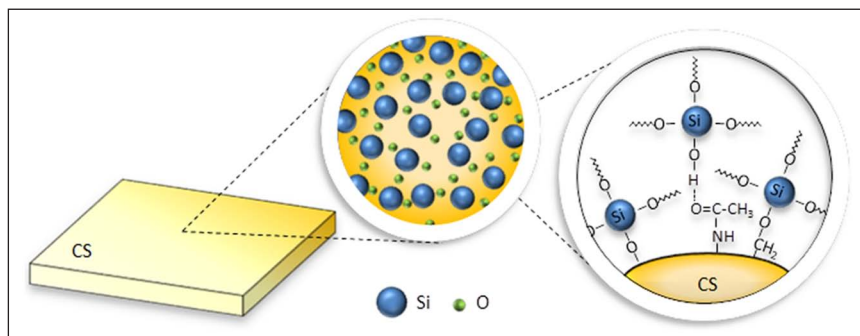


**Figure 6.** Illustrative representation of chitosan/soy protein hybrid (CSH) membranes.

and amino acids on soy protein.<sup>35</sup> Moreover, during formation of the hybrid membranes prepared by varying the ratio of TEOS:HCl, a competitive reaction can take place between the inorganic phase and organic components in the blended system, which may promote a variation in the inorganic incorporation, as observed by FTIR and XPS analyses. The small differences in the Si content in the CSH membranes can be associated to the initial heterogeneity of CS-blended system and to the TEOS:HCl ratios used. The differences observed in the %N and %C indicated that the C–N bonds in the material were substituted by Si–C bonds and, to a certain extent, by Si–O bonds. These findings imply that the CSH membranes were formed by organic phase entrapment of discrete inorganic moieties to form a blended system. An illustrative representation of the CSH membranes is shown in Figure 6.

Furthermore, the presence of residual silanol (Si–OH) groups (common in many sol–gel-derived materials) was detected in the membranes, indicating incomplete polycondensation.<sup>27</sup> It is also known that the presence of Si–OH groups in different types of materials can induce the formation of a bone-like apatite layer.<sup>36</sup> Therefore, these hybrid membranes could exhibit a bioactive behaviour that would be dependent on the amount and arrangement of silanol groups in the material structure.<sup>37</sup> Even with the variation in the inorganic incorporation, it is apparent by AFM analysis that this phase is well dispersed within the membranes. The intermolecular specific interactions (e.g. hydrogen bonding) in a hybrid system, which are considered to be the driving force for miscibility in non-covalently bonding hybrids, are responsible for the decreased phase separation.<sup>38</sup>

A positive effect of the incorporation of silica network was observed on the degradation and wettability of the membranes. A decrease in contact angle was attributed to the high concentration of Si–OH and Si–O–Si groups on the hybrid surfaces. Both hybrid membranes (CSH1 and CSH2) had significantly higher superficial energy ( $\gamma$ ) values indicating the generation of more reactive surface, which could in turn influence the cell–membrane interactions. Li et al.<sup>39</sup> reported that changes in contact angle of poly(dimethylsiloxane) (PDMS)-based hybrid materials could be related to localization of SiO<sub>2</sub> groups at the surface and/or outermost layer of the material. In addition, the existence of the mentioned groups could also be effective in the reduction of both swelling and weight loss with time, as shown in Figure 5. In fact, the introduction of an inorganic phase may restrain the blend component (CS protein) network from swelling due to the contraction effects arising from the silica bridging bonds.

Ren et al.<sup>9</sup> reported that the swelling of gelatin–siloxane hybrids could be controlled by an inorganic phase. One of the main objectives of this work was to overcome the recognized drawback of immiscibility associated with the CS protein system. The controlled swelling and degradation observed for the CSH hybrid membranes would indicate that an increase in the interactions between the blended components (CS protein) was achieved.

The result of incorporating an inorganic network into the CS system is also evident in the structural reinforcement to the matrices, which is reflected by the increase in  $E'$  (Figure 5(a)). Kim et al.<sup>40</sup> reported that hybrids with a small amount of silica may exhibit an improvement in mechanical properties for two reasons:<sup>38</sup> (1) the silica dispersion throughout the polymeric matrix and (2) the strong interaction between the polymer chain and silica or silanol groups through hydrogen bonding. A small amount of siloxane domains in the membrane formulation favorably changed the surface topography, hydrophilic/hydrophobic balance of the matrix and mechanical properties, which positively affect the cellular behaviour of the CSH membranes.

To evaluate the suitability of the CSH membranes for possible biomedical applications, cytotoxicity assessments of both CS and CSH extracts were carried out as a preliminary approach to assessing their potential toxicity. Based on the results obtained, it may be assumed that CSH membranes have extremely low cytotoxicity on cells, which supports the concept that these materials could be used in contact with the body. The differences in activity of these materials on diverse matrices may be due to variation in their composition. In addition, the CSH1 membranes had good degradability and mechanical properties favoring their use in guided tissue regeneration. In addition, CSH2 membranes could be used for long-term wound healing, during which the membranes will be resorbed by the body during the healing process.

## Conclusion

The presence of silica domains, randomly dispersed in the CSH membranes, contributed to the formation of CSH membranes with higher surface roughness in comparison with the unmodified CS membranes. The hybrid membranes were formed by an organic phase (CS blend) with entrapped discrete inorganic moieties. These hybrid structured membranes had slower degradability and better mechanical properties. It appears that even at a small amount of siloxane bonds, the CS system could display significant and specific interactions between the blended components. As result, these hybrid structured membranes had slower degradability and better mechanical properties. The low cytotoxicity levels of the membrane extracts are encouraging for future biocompatibility studies. The CS protein–based membranes could potentially be used for a variety of biomedical applications, such as guided bone regeneration strategies and wound dressing.

## Acknowledgements

The authors are thankful fo Dr GM Luz (3Bs Research Group, Portugal) for the illustrations.

## Declaration of conflicting interest

The authors declare that there is no conflict of interest.

## Funding

This work was financially supported by the Portuguese Foundation for Science and Technology – FCT (Grant SFRH/BPD/45307/2008, SFRH/BPD/21786/2009, SFRH/BPD/39331/2007 and SFRH/BD/64601/2009),

'Fundo Social Europeu' – FSE and 'Programa Diferencial de Potencial Humano – POPH' and was partially supported by the FEDER through POCTEP 0330\_IBEROMARE\_1\_P.

## References

- Kickelbick G. Introduction to hybrid materials. In: Kickelbick G (ed.) *Hybrid materials synthesis, characterization, and applications*. Weinheim: Wiley-VCH Verlag GmbH & Co; KGaA, 2007, pp. 1–48.
- Vasudevan P, Thomas S, Biju P, et al. Synthesis and structural characterization of sol-gel derived titania/poly(vinyl pyrrolidone) nanocomposites. *J Sol-Gel Sci Technol* 2012; 62: 41–46.
- Barbadillo M, Casero E, Petit-Dominguez M, et al. Surface study of the building steps of enzymatic sol-gel biosensors at the micro- and nano-scales. *J Sol-Gel Sci Technol* 2011; 58: 452–462.
- Silva S, Ferreira R, Fu L, et al. Functional nanostructured chitosan-siloxane hybrids. *J Mater Chem* 2005; 15: 3952–3961.
- Tian X, Wei F, Wang T, et al. Blood-brain barrier transport of Tat peptide and polyethylene glycol decorated gelatin-siloxane nanoparticle. *Mater Lett* 2012; 68: 94–96.
- Mahony O, Tsigkou O, Ionescu C, et al. Silica-gelatin hybrids with tailorable degradation and mechanical properties for tissue regeneration. *Adv Funct Mater* 2010; 20: 3835–3845.
- Eglin D, Perry CC and Ali SAM. A new class II poly ( $\epsilon$ -caprolactone)-silica hybrid: synthesis and in vitro apatite forming ability. *J Bioact Compat Pol* 2005; 20(5): 437–454.
- Shchipunov Y. Sol-gel-derived biomaterials of silica and carrageenans. *J Colloid Interface Sci* 2003; 268: 68–76.
- Ren L, Tsuru K, Hayakawa S, et al. Synthesis and characterization of gelatin-siloxane hybrids derived through sol-gel procedure. *J Sol-Gel Sci Technol* 2001; 21: 115–121.
- Silva SS, Mano JF and Reis RL. Potential applications of natural origin polymer-based systems in soft tissue regeneration. *Crit Rev Biotechnol* 2010; 30: 200–221.
- Peptu CA, Buhus G, Popa M, et al. Double cross-linked chitosan-gelatin particulate systems for ophthalmic applications. *J Bioact Compat Pol* 2010; 25(1): 98–116.
- Grech JMR, Mano JF and Reis RL. Chitosan beads as templates for layer-by-layer assembly and their application in the sustained release of bioactive agents. *J Bioact Compat Pol* 2008; 23(4): 367–380.
- Silva SS, Motta A, Rodrigues MT, et al. Novel genipin-cross-linked chitosan/silk fibroin sponges for cartilage engineering strategies. *Biomacromolecules* 2008; 9(10): 2764–2774.
- Silva S, Oliveira J, Mano J, et al. Physicochemical characterization of novel chitosan-soy protein/TEOS porous hybrids for tissue engineering applications. *Mater Sci Forum* 2006; 514–516: 1000–1004.
- Silva SS, Santos MI, Coutinho OP, et al. Physical properties and biocompatibility of chitosan/soy blended membranes. *J Mater Sci Mater Med* 2005; 16: 575–579.
- Silva SS, Goodfellow BJ, Benesch J, et al. Morphology and miscibility of chitosan/soy protein blended membranes. *Carbohydr Polym* 2007; 70(1): 25–31.
- Signini R and Campana Filho S. Characteristics and properties of purified chitosan in the neutral, acetate and hydrochloride forms. *Polimeros* 2001; 11: 58–64.
- Hirai A, Odani H and Nakajima A. Determination of degree of deacetylation of chitosan by  $^1\text{H}$  NMR spectroscopy. *Polym Bull* 1991; 26: 87–94.
- Vigano C, Manciu L, Buyse F, et al. Attenuated total reflection IR spectroscopy as a tool to investigate the structure, orientation and tertiary structure changes in peptides and membrane proteins. *Biopolymers* 2000; 55(5): 373–380.
- Nizhenko VI, Eremenko VN and Sklyarenko LI. Application of the sessile drop method to the determination of the surface energy and density of liquids wetting the backing material. *Powder Metall Met Ceram* 1965; 4(6): 463–466.
- Owens DK and Wendt RC. Estimation of the surface free energy of polymers. *J Appl Polym Sci* 1969; 13: 1741–1747.
- Prigent H, Pellen-Mussi P, Cathelineau G, et al. Evaluation of the biocompatibility of titanium-tantalum alloy versus titanium. *J Biomed Mater Res* 1998; 39(2): 200–206.
- ISO/10993:1992. Biological evaluation of medical devices Part 5: Tests for in vitro cytotoxicity, (ISO 10993-5:2009).
- Gomes ME, Reis RL, Cunha AM, et al. Cytocompatibility and response of osteoblastic-like cells to starch-based polymers: effect of several additives and processing conditions. *Biomaterials* 2001; 22(13): 1911–1917.
- Pawlak A and Mucha M. Thermogravimetric and FTIR studies of chitosan blends. *Thermochim Acta* 2003; 396(1–2): 153–166.
- Subirade M, Kelly I, Guéguen J, et al. Molecular basis of film formation from a soybean protein: comparison between the conformation of glycinin in aqueous solution and in films. *Int J Biol Macromol* 1998; 23(4): 241–249.

27. de Zea Bermudez V, Carlos LD and Alcácer L. Sol-gel derived urea cross-linked organically modified silicates. I. Room temperature mid-infrared spectra. *Chem Mater* 1999; 11: 569–580.
28. Osswald J and Fehr KT. FTIR spectroscopic study on liquid silica solutions and nanoscale particle size determination. *J Mater Sci* 2006; 41: 1335–1339.
29. Matienzo L and Winnacker SK. Dry processes for surface modification of a biopolymer: chitosan. *Macromol Mater Eng* 2002; 287: 871–880.
30. Eick JD, Good RJ and Neumann AW. Thermodynamics of contact angles. II. Rough solid surfaces. *J Colloid Interf Sci* 1975; 53(2): 235–248.
31. Mano J. Viscoelastic properties of chitosan with different hydration degrees as studied by dynamic mechanical analysis. *Macromol Biosci* 2008; 8(1): 69–76.
32. Uragami T, Katayama T, Miyata T, et al. Dehydration of an ethanol/water azeotrope by novel organic-inorganic hybrid membranes based on quaternized chitosan and tetraethoxysilane. *Biomacromolecules* 2004; 5: 1567–1574.
33. Ayers MR and Hunt AJ. Synthesis and properties of chitosan-silica hybrid aerogels. *J Non-Cryst Solids* 2001; 285: 123–127.
34. Mukkamala R and Cheung H. Acid and base effects on the morphology of composites formed from microemulsion polymerization and sol-gel processing. *J Mater Sci* 1997; 32: 4687–4692.
35. Vaz CM, Graaf LA, Reis RL, et al. Soy protein-based systems for different tissue regeneration applications. In: Reis RL and Cohn D (eds) *Polymer based systems on tissue engineering, replacement and regeneration*. Dordrecht, The Netherlands: Kluwer Academic Publishers, 2002, pp. 93–110.
36. Leonor IB, Baran ET, Kawashita M, et al. Growth of a bonelike apatite on chitosan microparticles after a calcium silicate treatment. *Acta Biomater* 2008; 4: 1349–1359.
37. Kokubo T, Kim HM and Kawashita M. Novel bioactive materials with different mechanical properties. *Biomaterials* 2003; 24: 2161–2175.
38. Li R, Nie K, Pang W, et al. Morphology and properties of organic-inorganic hybrid materials involving TiO<sub>2</sub> and poly(-caprolactone), a biodegradable aliphatic polyester. *J Biomed Mater Res A* 2007; 83(1): 114–122.
39. Li Z, Han W, Kozodaev D, et al. Surface properties of poly(dimethylsiloxane)-based inorganic/organic hybrid materials. *Polym* 2006; 47(4): 1150–1158.
40. Kim DS, Park HB, Lee YM, et al. Preparation and characterization of PVDF/silica hybrid membranes containing sulfonic acid groups. *J Appl Polym Sci* 2004; 93: 209–218.